Spatial cooperativity in microchannel flows of soft jammed materials: A mesoscopic approach

Alexandre Nicolas, Jean-Louis Barrat

Laboratoire Interdisciplinaire de Physique,

Université Joseph Fourier Grenoble, CNRS UMR 5588,

BP 87, 38402 Saint-Martin d'Hères, France

(Dated: December,10^{th} 2012)

Abstract

The flow of amorphous solids results from a combination of elastic deformation and local structural rearrangements, which induce non-local elastic deformations. These elements are incorporated into a mechanically-consistent mesoscopic model of interacting elastoplastic blocks. We investigate the specific case of channel flow with numerical simulations, paying particular attention to situations of strong confinement. We find that the simple picture of plastic events embedded in an elastic matrix successfully accounts for manifestations of spatial cooperativity. Shear rate fluctuations are observed in seemingly quiescent regions, and the velocity profiles in confined flows at high applied pressure deviate from those expected in the absence of nonlocal effects, in agreement with experimental data. However, we suggest a different physical origin for the large deviations observed when walls have rough surfaces, associated with "bumps" of the particles against the asperities of the walls.

Shear waves are damped in liquids, and propagate in elastic solids. This well-established distinction has major implications in the field of seismology [1], but also has bearing on the peculiar nonlocal rheology of soft jammed/glassy materials, which share solid (elastic) and liquid (flow) properties.

In fact, the flow of these materials bears notable similarities with earthquakes: it features a solid-like behavior at rest and local yielding above a given applied stress. Yielding is characterized by the emergence of local "shear transformations" [2] involving a few particles [3], associated with a local fluidization of the material. These structural rearrangements, hereafter named plastic events, induce long-range deformations. The microscopic details vary to some extent with the particular nature of the material. In the case of foams, they are identified as T1 events [4] in which the local change of neighbors is mediated by an unstable stage with four bubbles sharing one vertex. The robustness of the scenario for an extremely wide range of materials is striking. Ample evidence of the local plastic events and their long-range effects is indeed provided both by experiments using diverse materials [3, 5, 6] and by simulations [7, 8].

Turning to the specific case of channel flow, the existence of long-range interactions render any purely local approach questionable in a system featuring an inherently inhomogeneous shear and specific boundary conditions due to the walls. Convincing experimental evidence disproves the very *existence* of a local constitutive relation $\sigma = \sigma\left(\dot{\gamma}\right)$ [9], where $\dot{\gamma}$ and σ are the local shear rate and shear stress. The presence of nonlocal effects highlights the effect of spatial cooperativity. These observations were rationalized in [9, 10] by introducing a diffusion equation for the local fluidity $f = \dot{\gamma}/\sigma$:

$$\xi^2 \Delta f - (f - f_{bulk}(\sigma)) = 0, \tag{1}$$

Here ξ is a cooperativity length, and f_{bulk} is the local bulk fluidity, measured in a homogeneous, simple shear situation. Eq.1 has been tested with considerable success [11, 12]. However, the approach ignores the fluctuating nature of plastic deformation, and relies on experimental measurements of the boundary conditions.

Mesoscopic models [13–15] offer a computationally-efficient way to recover part of the complexity of the dynamics, while leaving behind microscopic details. Most importantly, they allow us to test our understanding of the physical processes involved in the flow, and identify relevant parameters for its description [15]. However, direct comparison with ex-

perimental data is scarce.

In this Letter, we build upon previous work [14, 15] to develop a simple, but mechanically consistent, 2D tensorial mesoscopic model that incorporates the phenomenology reported above, as well as (coarsened) convection. For the first time such a model is used to simulate a channel flow, and its predictions are compared to experimental data.

The channel is modeled as a rectangular elastic matrix, which is spatially discretized into a regular lattice of square-shaped blocks. Under the assumption of isotropy and incompressibility, Hooke's law states that the deviatoric stress tensor $\boldsymbol{\sigma}$ is proportional to the local strain tensor $\boldsymbol{\epsilon}$,

$$\sigma_{xx} = \mu\left(\epsilon_{xx} - \epsilon_{yy}\right) = 2\mu\epsilon_{xx} \;; \quad \sigma_{xy} = 2\mu\epsilon_{xy}. \tag{2}$$

μ is the shear modulus, and x and y are the flow and gradient directions, respectively. The system covers the domain $(x, y) \in [0, L_x] \times [0, L_y]$, with L_x and L_y the channel length and width. The initial response of the material confined in a channel to an applied pressure gradient $\nabla p\, e_x$ is therefore given by: $\sigma_{xy}\left(x, y, t = 0\right) = \nabla p \;\; (y - {}^{L_y}\!/_2)$ and $\sigma_{xx}\left(x, y, t = 0\right) = 0$.

As soon as a yielding criterion is met in a block, the block undergoes a plastic event, during which the stored elastic energy is dissipated. Within the framework of eigenstrain theory [16], the elastic strain $\boldsymbol{\epsilon}$ is converted into a plastic eigenstrain $\boldsymbol{\epsilon^{pl}}$. Physically, this corresponds to the change of reference elastic configuration following particle rearrangement. The conversion takes a finite time, due to dissipative effects.

Since the block is embedded in an elastic matrix, the localized eigenstrain $\boldsymbol{\epsilon^{pl}}$ induces an elastic field $\boldsymbol{\sigma}^{(1)}\left(r\right) = \int \boldsymbol{\mathcal{G}}\left(r, r'\right) \cdot 2\mu\boldsymbol{\epsilon^{pl}}\left(r'\right) dr'$, where the elastic propagator $\boldsymbol{\mathcal{G}}$ depends on the boundary conditions. The assumption of an underlying elastic behavior is bolstered by the similarity of the induced field with experimental and numerical observations [3, 8], all of which exhibit a quadrupolar angular dependence and a $\|r - r'\|^{-d}$-like decay in d dimensions. Combining the different elements, one gets the equation of evolution of a block:

$$\partial_t \boldsymbol{\sigma}\left(r\right) = \dot{\boldsymbol{\Sigma}}^{\boldsymbol{ext}}\left(r\right) + \int \boldsymbol{\mathcal{G}}\left(r, r'\right) \cdot 2\mu\dot{\boldsymbol{\epsilon}}^{\boldsymbol{pl}}\left(r'\right) d^2r' \tag{3}$$

Here, $\dot{\boldsymbol{\epsilon}}^{\boldsymbol{pl}} = \frac{1}{\tau}\boldsymbol{\epsilon}$ if the block is plastic, $\dot{\boldsymbol{\epsilon}}^{\boldsymbol{pl}} = 0$ otherwise, and τ is the characteristic timescale for the release of the stored elastic stress. $\dot{\boldsymbol{\Sigma}}^{\boldsymbol{ext}}$ is the time-derivative of the stress response of a purely elastic material to the same applied conditions; therefore $\dot{\boldsymbol{\Sigma}}^{\boldsymbol{ext}} = 0$ if the flow is

pressure-driven. Numerically, at each time step, Eq.3 is solved in Fourier space, on a finer grid where, for accuracy, each block is divided into four subcells.

There is obviously some arbitrariness regarding the choice of the yielding criterion and the duration of plastic events. The corresponding switching rates are denoted by $l(\sigma)$ and $e(\sigma)$,

$$\text{elastic regime} \underset{e(\sigma)}{\overset{l(\sigma)}{\rightleftharpoons}} \text{plastic event.}$$

The probability to yield $l(\sigma)$ is set to $l(\sigma) = \Theta(\sigma - \sigma_{\mu y}) \exp\left(\frac{\sigma-\sigma_y}{x_l}\right)\tau^{-1}$, where Θ is the Heaviside function and $\sigma = \|\boldsymbol{\sigma}\|$, so as to mimic an activated process of *non-cooperative* origin, associated with a material-dependent intensive parameter x_l. Imposing a finite critical stress $\sigma_{\mu y}$, below which no plastic event can occur, is crucial for the existence of a macroscopic yield stress $\sigma(\dot{\gamma} \to 0) \neq 0$. Also note that the von Mises yield criterion is recovered in the limit $x_l \to 0$. The above expression accounts for the long-time relaxation of a pre-sheared material, observed even in the case of (athermal) granular materials [17]. We assume that elasticity is restored when the plastic deformation rate becomes low, and choose: $e(\sigma) = \exp\left(\frac{\sigma_{\mu y}-\sigma}{x_e}\right)\tau^{-1}$, where we have introduced another material parameter, x_e.

Walls are modeled by imposing no-slip boundary conditions at $y = 0$ and $y = L_y$. This results in a lengthy expression for the propagator, which we defer to a longer publication, along with details of the derivation. It is however noteworthy that, for a given eigenstrain $\dot{\boldsymbol{\epsilon}}^{\boldsymbol{pl}}$, the elastic stress that is released locally is up to 35% larger than in the bulk if the plastic event occurs near a wall.

Finally, a coarsened picture of convection is implemented, whereby lines of blocks in the flow direction (instead of individual blocks) are incrementally shifted.

We choose units of time and stress such that $\tau = 1$, $\mu = 1$ and we set $\sigma_y = 1$. The remaining model parameters, $\sigma_{\mu y}$, x_l, and x_e, are now fitted by comparing the predictions of the model in simple shear flow, i.e., $\sigma(t = 0) = 0$ and $\dot{\Sigma}^{ext} = \mu\dot{\gamma}_{app}$ in Eq.3, where $\dot{\gamma}_{app}$ is the applied shear rate, with the macroscopic rheology measurements collected by Goyon and co-workers [9, 12] for an oil-in-water emulsion of average radius $6.5\,\mu$m , which follows a Herschel-Bulkley law $\sigma = \sigma_0 + A\dot{\gamma}^n$, $n \approx 0.5$. The inset of Fig.3 shows that the experimental data can satisfactorily be reproduced with our model by using the following parameters: $\sigma_{\mu y}$=0.17, $x_l = 0.249$, and $x_e = 1.66$. Note that the model units of stress and time have been appropriately rescaled.

Cooperativity is a general feature of the flow of amorphous solids, regardless of the flow geometry and the driving. Channel flow, however, is specific in that

(i) the non-locality of the stress redistribution couples streamlines subject to *different* shear stresses.

(ii) the presence of a wall, whether it be rough or smooth, may create a specific surface rheology, different from that in the bulk.

In practice, these effects are of primary importance for confined flows in microchannels, but they are not intrinsically caused by confinement.

Let us first consider Point (i). To estimate its importance, we introduce a dimensionless number, the Babel number $\mathcal{B}a \equiv \delta f / f_{bulk}(\sigma)$, where $\delta f = f - f_{bulk}$ is the deviation from the expected fluidity profile owing to cooperative effects between regions subject to different driving forces. Within the theoretical framework of fluidity diffusion, Eq. 1, and for a fluid obeying a Herschel Bulkley relation in the bulk, it can be shown that $\mathcal{B}a = \left(\xi \frac{\|\nabla\sigma\|}{\sigma-\sigma_0}\right)^2 = \left(\xi \frac{\|\nabla p\|}{\sigma-\sigma_0}\right)^2$ (in regions where the locally imposed stress σ is larger than the yield stress σ_0). Large deviations from bulk behavior are expected when the stress is close to the yield value. A striking consequence of this first point was very recently unveiled by Jop *et al.* [11] in a system similar to that of Goyon *et al.* [12]. They analyzed experimental data for an oil-in-water emulsion in an almost two-dimensional microchannel flow, and showed that the seemingly quiescent, rigid plug is in fact subject to finite shear rate fluctuations $\delta\dot{\gamma}(x,y) = \sqrt{\langle \dot{\gamma}(x,y)^2 \rangle - \langle \dot{\gamma}(x,y) \rangle^2}$, where the brackets denote time averages. This clearly points to a nonlocal effect of the sheared regions.

We now compare the model results[18] directly to experimental data: Fig.1 shows the velocity profiles [19], and Fig.2 shows the corresponding shear rate fluctuation profiles, for a numerical channel of transverse size $N_y = 16$ blocks.

Although the parameters of the model have been constrained only weakly by adjusting the macroscopic flow curve, semi-quantitative agreement is observed in regions far from the walls - apart from the large discrepancy at the highest applied pressure. The discrepancies in the vicinity of the walls will be considered below. It is interesting to note that the fitted channel size provides an estimate for the linear size $N_\varnothing$ of an elastoplastic block measured in particle diameters, $N_\varnothing \approx 2$.

Not only shear rate fluctuations, but also the average shear rate, elude a local, or bulk, description, when $\mathcal{B}a$ gets large. This paradigm-shifting fact is the major result of experi-

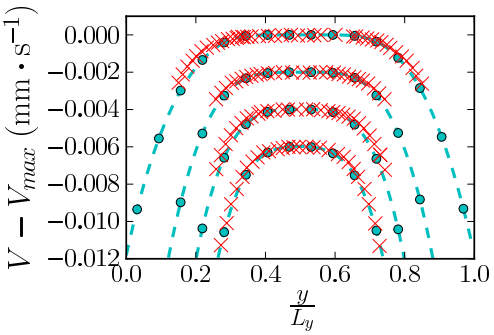

Figure 1. Offset velocity as a function of the channel crosswise coordinate, for stresses at the wall σ_w =141 Pa, 188 Pa, 235 Pa, 282 Pa, corresponding to σ_w = 0.36, 0.48, 0.60, 0.72 in model units, from top to bottom. (×) Experimental data collected by Jop *et al.* [11] (channel width: 225 μm), (•) numerical results for a channel of $N_y = 16$ blocks crosswise. The curves are offset with respect to each other for clarity.

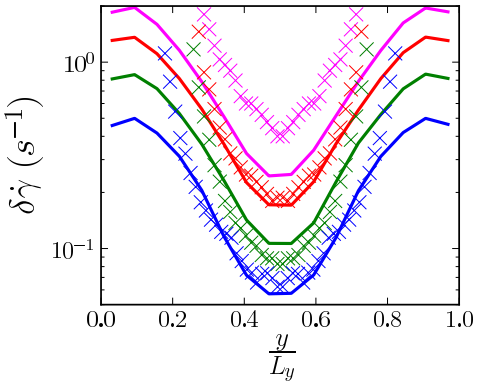

Figure 2. Shear rate fluctuations $\delta\dot{\gamma}(y)$ (averaged along the x-direction), for σ_w =141 Pa, 188 Pa, 235 Pa, 282 Pa (identical to Fig.1), from bottom to top. (×) Experimental data collected by Jop *et al.* [11], (*solid lines*) numerical results for $N_y = 16$.

mental observations by Goyon and co-workers in microchannel flows of emulsions with either smooth or rough walls [9].

In the case of smooth walls, deviations from the macroscopic bulk constitutive relations are comparatively weak. In contrast to strain rate fluctuations, they become perceptible only at high applied pressures in confined geometries, when the stress at the wall is larger than some channel-size dependent critical value $\sigma_w^\star$. Under these conditions, the overall fluidity of the system is enhanced. Consistently with our expression of the Babel number,

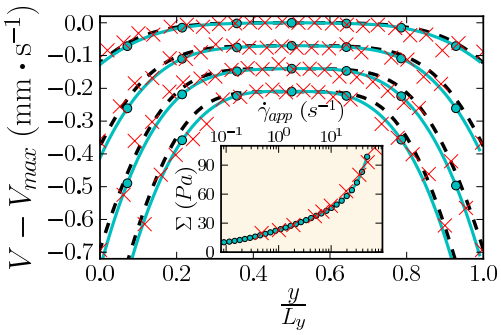

Figure 3. Velocity profiles in the microchannel. The curves are shifted for clarity. (×) Experimental measurements by Goyon *et al.* [12] for (from top to bottom) $\sigma_w = 45$, 60, 75, 91 Pa, i.e., $\sigma_w = 0.75$, 1.0, 1.25, 1.52 in model units, in a 112 μm-wide smooth channel; (•) numerical results for $N_y = 7$. (The solid line is a guide to the eye); *dashed black line*: predicted velocity profile on the basis of the macroscopic flow curve $\Sigma(\dot{\gamma}_{app})$, shown in the *inset* graph ((×) experimental data from [12]; (•) numerical results in a large system, $N_y = 64$).

the most prominent discrepancies with the bulk predictions are observed near the edges of the plug, which become more rounded. Accordingly, cooperativity can soften the material so that it flows even below the macroscopic yield stress. This aspect is corroborated by numerical simulations [20], and is expected within the framework of the fluidity diffusion equation [10]. Fig.3 shows that our model also satisfactorily captures these features. For the critical wall stresses $\sigma_w^\star$ to coincide between the model and the experiments, the transverse size of the numerical channel must be set between 6 and 10 blocks, which again corresponds to $N_\varnothing \approx 2$. Besides, for such transverse microchannel sizes, the maximal velocity displays large oscillations in time, as has often been reported experimentally[21].

Let us now turn to a comparison with a description in terms of fluidity diffusion, Eq. 1. To solve Eq. 1, the shear-rate dependence of the length ξ must be specified, and two boundary conditions (BC) are required. Regarding the BC, we impose $f(y = 0) = f(y = L_y)$, and set the fluidity at a point close to the wall to the value measured in simulations. For the fluidity dependence of ξ, two cases are studied in Fig.4: either no dependence, i.e., $\xi = \xi_0$, following Goyon *et al.* [9], or a power-law dependence, $\xi(\dot{\gamma}) = \xi_0 \dot{\gamma}^{-0.25}$, where $\dot{\gamma}$ is the product of the local shear stress and fluidity, as derived in Ref. [10] in the limit $\dot{\gamma} \to 0$, and in reasonable agreement with the data of Ref. [11]. In both cases, ξ_0 is adjusted by a least square minimization. Overall, the power-law dependence provides a closer fit of our numerical

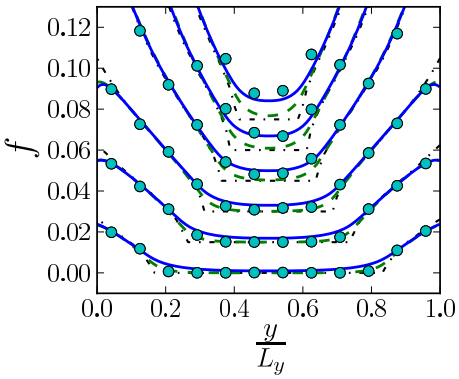

Figure 4. Fluidity profiles for $N_y = 12$. Filled circles: numerical results, dashed green line: solution of Eq.1 with $\xi(\dot{\gamma}) = 0.03702$, solid blue line: solution of Eq.1 with $\xi(\dot{\gamma}) = 0.01146\,\dot{\gamma}^{-0.25}$. The thin dash-dotted lines represent the bulk fluidity f_{bulk}.

results, especially at higher applied pressures. However, neither assumption concerning $\xi(\dot{\gamma})$ was able to provide a perfect fit, a defect that we ascribe to the approximation of long-range interactions by a diffusive term, and to the neglect of fluidity fluctuations.

Now, when rough walls are substituted for smooth walls, the situation differs widely. Much larger deviations are observed, even at lower Babel numbers than above. The discrepancies caused by the change of the surface roughness of the walls point to the prevalence the specific surface rheology, point (ii) above. Further evidence comes from the fact that deviations are particularly large close to the walls. The no-slip BC at the wall imposed in our model are insufficient to account for these large deviations. One is therefore led to conclude that either (a) the roughness of the wall alters the structure of the material in its vicinity or (b) slip along the wall generates a stress field in the system, as particles constantly bump into wall asperities.

Since the observed deviations are not restricted to the direct vicinity of the (rough) walls, we examine the second possibility here, namely slip along the wall as a source of mechanical noise. Goyon *et al.* [9] measured wall slip both for smooth and rough surfaces, the latter having asperities of a characteristic lengthscale of $1\,\mu$m, whereas the emulsion is made of $\sim 6\,\mu m$-diameter droplets. In the case of smooth surfaces, asperities are too small to deform the particles significantly, and the presence of wall slip is therefore unlikely to induce considerable change as compared to the no-slip case, which validates our approach. On the contrary, wall slip along a rough surfaces brings about "bumps" (or deformations)

of the particles into surface asperities. Similarly to bulk plastic events, these "bumps" are expected to induce an elastic field in the material. This scenario has the potential to explain why deviations are not always observed in nominally similar conditions: Seth and co-workers [22], for instance, used a different surface preparation protocol to obtain rough surfaces and did not detect any nonlinearity of the flow in the vicinity of the rough walls, but, quite interestingly, they also reported that wall slip remained negligible in that case.

Our model cannot render the mechanical effects of wall slip along a rough surface without further input. Nevertheless, fictitious plastic events can artificially be added along the walls to mimic the impact of "bumps". Concretely, we now model both walls as lines of blocks and select a fraction ($1/3$) of these blocks at random as mechanical noise sources, that is to say, they shall release a constant plastic strain $\dot{\epsilon}_{xy}^{fict\,pl}$ (≈ 5) by unit time. It should be remarked that the procedure does on no account violate mechanical equilibrium. The resulting local flow curves, shown as Supplemental Material, are qualitatively similar to those obtained experimentally in Ref. [9]. Let us also remark that shear rate profiles in the presence of fictitious plastic events do not flatten in the vicinity of the walls (*data not shown*), as in Fig.2, and are therefore more compatible with the experimental data.

In conclusion, we have refined and extended a mesoscopic model based on a default elastic behavior and finite-time plastic events to simulate a confined channel flow. We have realized the first direct comparison of such a model with experimental data, paying particular attention to manifestations of spatial cooperativity. It has been found that, the model accounts for the presence of shear-rate fluctuations in seemingly quiescent regions, and the local deviations from the macroscopic flow curve when the inhomogeneity of the driving, quantified by the Babel number, is large. The comparison with experimental data also provided us with an estimate of the size of an elastoplastic block, $N_{\varnothing} \approx 2$, roughly in agreement with experimentally-measured values of the size of a shear transformation [3]. These successes of the mesoscopic model are encouraging for further studies of statistical aspects of flow in complex fluids. The description in terms of fluidity diffusion is reasonable, but imperfect.

The much larger deviations observed in the presence of rough walls, on the other hand, are not described by a model that imposes a fixed velocity at the walls. This points to the contribution of another physical mechanism to the deviations. We hypothesize that the bumps of the particles against the surface asperities due to wall slip, and the long-range

elastic deformations they induce, may be at its source. Further experimental and numerical studies of wall rheology will be needed to quantify this mechanism.

AN & JLB thank K. Martens, D. Rodney, L. Bocquet and P. Chaudhuri for interesting discussions, and A. Colin for sending the experimental data. AN acknowledges a fruitful discussion with R. Besseling, JLB is supported by Institut Universitaire de France and by grant ERC-2011-ADG20110209.

[1] P. Shearer, *Introduction to Seismology* (Cambridge University Press, 1999) p. 272.

[2] A. Argon, Acta metallurgica **27**, 47 (1979).

[3] P. Schall, D. A. Weitz, and F. Spaepen, Science (New York, N.Y.) **318**, 1895 (2007).

[4] H. Princen, Journal of Colloid and Interface Science **105**, 150 (1985).

[5] A. Amon, V. B. Nguyen, A. Bruand, J. Crassous, and E. Clément, Physical Review Letters **108**, 135502 (2012).

[6] K. Nichol and M. van Hecke, Physical Review E **85**, 061309 (2012).

[7] M. L. Falk and J. S. Langer, Physical Review E **57**, 7192 (1998).

[8] A. Lemaître and C. Caroli, Physical Review E **76**, 036104 (2007).

[9] J. Goyon, A. Colin, G. Ovarlez, A. Ajdari, and L. Bocquet, Nature **454**, 84 (2008).

[10] L. Bocquet, A. Colin, and A. Ajdari, Physical review letters **103**, 036001 (2009).

[11] P. Jop, V. Mansard, P. Chaudhuri, L. Bocquet, and A. Colin, Physical Review Letters **108**, 148301 (2012).

[12] J. Goyon, A. Colin, and L. Bocquet, Soft Matter **6**, 2668 (2010).

[13] J. Baret, D. Vandembroucq, and S. Roux, Physical review letters **89**, 195506 (2002).

[14] G. Picard, A. Ajdari, F. Lequeux, and L. Bocquet, Physical Review E **71**, 010501 (2005).

[15] K. Martens, L. Bocquet, and J. Barrat, Soft Matter **8**, 4197 (2012).

[16] T. Mura, *Micromechanics of Defects in Solids* (Springer, 1987) p. 587.

[17] R. R. Hartley and R. P. Behringer, Nature **421**, 928 (2003).

[18] Videos are provided as Supplemental Material.

[19] We have discarded the curves corresponding to the lowest two applied pressures in [11], because we are not sure of the accuracy of the measurements of the lowest shear rate fluctuations.

[20] P. Chaudhuri, V. Mansard, A. Colin, and L. Bocquet, Physical Review Letters **109**, 036001

(2012).

[21] L. Isa, R. Besseling, A. Morozov, and W. Poon, Physical review letters **102**, 58302 (2009).

[22] J. R. Seth, C. Locatelli-Champagne, F. Monti, R. T. Bonnecaze, and M. Cloitre, Soft Matter **8**, 140 (2012).

Supplementary material

FICTITIOUS PLASTIC EVENTS AS SOURCES OF MECHANICAL NOISE

To mimick the impact of the "bumps" into wall asperities induced by wall slip, we introduce fictitious plastic events along the wall. More precisely, we now model both walls as lines of blocks and select a fraction of these blocks at random as mechanical noise sources, that is to say, they shall release a constant plastic strain $\dot{\epsilon}_{xy}^{fict\,pl}$ by unit time. Fig.5 shows the resulting local flow curves for a fraction of fixed mechanical noise sources of 1/3 picked at random, and $\dot{\epsilon}_{xy}^{fict\,pl} = \pm 4.5$.

VIDEOS SHOWING THE SPATIOTEMPORAL DYNAMICS

Files *Video0p75.mpg* and *Video0p48.mpg* are videos representing the succession of plastic events in a channel flow.

The system flows along the horizontal direction, towards the right, and the flow is confined between two horizontal walls, at the top and at the bottom. A plastic event is depicted as a coloured square that gradually fades into black as the plastic event comes to an end.

The color of the plastic event represents its principal direction, *ie* the yielding angle: Blocks that yield in the macroscopic shear direction, ie $\dot{\epsilon}_{xx}^{pl} = 0$ and $\dot{\epsilon}_{xy}^{pl} \neq 0$, are painted in red, while plastic events with $\dot{\epsilon}_{xx}^{pl} \neq 0$ and $\dot{\epsilon}_{xy}^{pl} = 0$ are represented in blue. A color gradient is applied between these limiting cases.

Video0p75.mpg shows a system of $N_y = 7$ blocks in the crosswise direction and $N_x = 64$ blocks in the streamwise direction (only half of the horizontal axis is shown). The stress imposed at the wall is $\sigma_w = 0.75$ in model units, and the other model parameters are identical to those used in the paper. The video covers a time span $\Delta t = 33.5$ in model units.

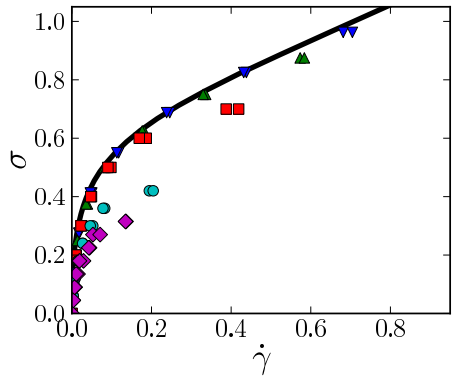

Figure 5. Local shear rate $\sigma\,(y)$ *vs* local shear rate $\dot{\gamma}\,(y)$ (averaged on streamlines $y = cst$) in the microchannel, when fictitious mechanical noise sources of intensity $\dot{\epsilon}_{xy}^{fict\,pl} = \pm 4.5$ are added on a fraction (1/3) of blocks on the wall lines. σ_w=(♦) 0.36, (●) 0.48, (■)0.8, (▲)1.0, (▼)1.1 in model units. Solid line: macroscopic flow curve.

Video0p48.mpg shows a system of $N_y = 16$ blocks in the crosswise direction and $N_x = 64$ blocks in the streamwise direction (only half of the horizontal axis is shown). The stress imposed at the wall is $\sigma_w = 0.75$ in model units, and the other model parameters are identical to those used in the paper. The video covers a time span $\Delta t = 28.3$ in model units.